

Nonlinear distortions of the angular spectrum in stimulated scattering

V. N. Belousov, L. A. Bol'shov, N. N. Elkin, N. G. Koval'skiĭ, Yu. K. Nizienko, and M. I. Persiantsev

I. V. Kurchatov Institute of Atomic Energy, Academy of Sciences of the USSR, Moscow

(Submitted 18 April 1986)

Zh. Eksp. Teor. Fiz. **92**, 61–73 (January 1987)

An experimental and theoretical study is reported of the relative contributions of individual mechanisms to the distortion of the angular spectrum of short light pulses in different nonlinear media. In absorbing media, the main source of energy transfer to weak angular modes is the thermal modulation of the refractive index, which leads to a uniform broadening of the angular spectrum. The distortion of the space-time structure of light pulses in nonabsorbing media is due to the combined effect of Kerr nonlinearity and striction, which is resonant in character.

I. INTRODUCTION

The transformation of the angular structure of radiation in stimulated scattering has recently become particularly topical in connection with the development of a number of applications based on stimulated Raman scattering (SRS) and stimulated Mandel'shtam-Brillouin scattering (SMBS). In problems involving the transformation of the frequency of excimer laser radiation in the blue-green part of the spectrum, and the compression of excimer laser pulses by resonant and nonresonant SRS, the effectiveness and quality of the transformed radiation depend on the nature of the nonlinear interaction of different angular modes, both in the pump field and the Stokes field. A related problem arises in attempts to elucidate basic limitations on the precision of wavefront reversal (WR) in SMBS. One of the main nonlinear processes is then energy transfer between angular components of the Stokes beam and the pump beam. Previous papers¹⁻⁹ have discussed a number of mechanisms for the nonlinear interaction between angular beam components, but the relative contribution of the individual mechanisms was not examined in detail. In this paper, we report an experimental and theoretical study of the contribution of individual mechanisms to the distortion of the angular structure, and formulate a number of recommendations designed to increase the degree of reproducibility in WR.

2. EXPERIMENT

In order to investigate the mechanisms responsible for distorting the angular structure of radiation scattered by an SMBS mirror, we have measured the Stokes radiation parameters as functions of time. The apparatus employed is illustrated schematically in Fig. 1. The exciting (pump) radiation was the second harmonic of a neodymium laser with the following output parameters: wavelength $\lambda = 0.527 \mu\text{m}$, energy $E \leq 2 \text{ J}$, beam diameter $d = 8 \text{ mm}$, pulse width at half-maximum $\tau = 15 \text{ ns}$, divergence $\theta = 3 \times 10^{-4} \text{ rad}$, and width of spectrum $\Delta\nu = 2 \times 10^{-3} \text{ cm}^{-1}$. The SMBS-active media employed in these experiments were acetone, ethyl alcohol, distilled water, and toluene. Coaxial detectors and a 6LOR oscillograph were used to measure the parameters of the SMBS mirror such as the reflection coefficient R and degree of reversal h , with a time resolution of about 1 ns. We note that the position of the spatial filter in the apparatus shown in Fig. 1 is particularly convenient because it ensures that the working and diagnostic apertures are always coinci-

dent. The weak angular components in the filtered pump beam are due to the re-reflection of the main beam by the surfaces of the beam-splitter and the input window of the cell, as well as imperfections in the focusing lens and noise in the hypersonic grating in the nonlinear medium.

The $R(t)$ and $h(t)$ curves shown in Fig. 2 were constructed by dividing the instantaneous pump power (signal from coaxial photocell 4) into the instantaneous Stokes power scattered by the SMBS mirror into the complete angular aperture of the focusing lens 6 (signal from coaxial photocell 3) and into the diffraction angle defined by the aperture 5 (signal from coaxial photocell 2). The pulses were locked together in time to within better than 1 ns. All the measurements were performed on the linear portion of the photocell characteristics.

The absolute reflection coefficient of the SMBS mirror was obtained by replacing it with an ordinary dielectric mirror. The following results were obtained in this way. When the pump energy exceeded the SMBS threshold by a factor of 5–10, the reflection coefficient for all the liquids that were investigated was found to depend on the instantaneous pump power, but was practically independent of time (curve 1, Fig. 2a). The degree of reversal did not change during the entire Stokes pulse. No noticeable changes appeared on the $R(t)$ curve when the pump energy was allowed to exceed the threshold by a factor of 50–100. However, the $h(t)$ curve did show significant changes. The change in the form of the $h(t)$ curve for high levels of pump radiation enabled us to divide the media under investigation into two categories. In some media, the degree of reversal decreased at the center of the pulse and then increased toward the end of the pulse. A typical example of this is shown by curve 2 in Fig. 2b. The reduc-

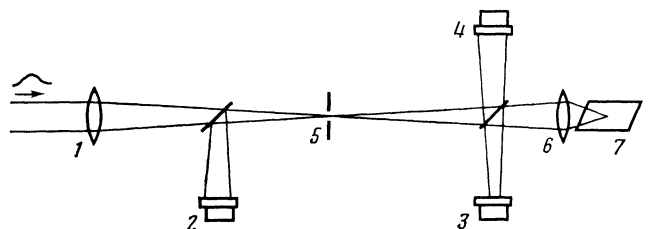


FIG. 1. Experimental setup: 1—lens, $f = 200 \text{ cm}$; 2,3,4—coaxial photocells; 5—aperture, 0.8 mm in diameter; 6—lens, $f = 5 \text{ cm}$; 7—cells containing the SMBS-active medium.

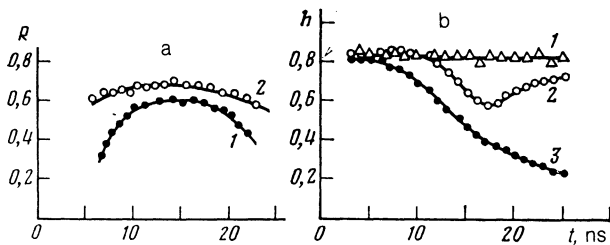


FIG. 2. Typical time dependence of the reflection coefficient R (a) and degree of WR h (b): 1—pump just above threshold, 2,3—pump well above threshold (2—water, alcohol, acetone, 3—toluene).

tion in the degree of reversal in such media was found to depend both on the ratio of pump power to SMBS threshold, and on the properties of the media under investigation. A monotonic deterioration in reversal with time was found to occur in other media (curve 3, Fig. 2b). The fact that the reduction in the degree of reversal occurred at practically constant reflection coefficient shows that the main contribution to the deterioration in the degree of reversal in these experiments is provided by energy transfer between angular components.

It is well-known (see, for example, Ref. 1) that energy transfer between two beams that is due to stimulated scattering (SS) occurs only when the relaxation time of the inhomogeneities induced in the medium, which are responsible for the interaction between the beams, exceeds the typical time scales of the light grating (pulse length in the case of different frequencies). Among the three different mechanisms responsible for SS (heating, electrostriction, and the Kerr effect),¹⁾ the first has the longest relaxation time: $\tau_T = \Lambda^2/4\pi^2\chi$, where χ is the thermal diffusivity and Λ is the spatial period of the light grating. Under the conditions of our experiments, $\Lambda \sim 0.1-0.01$ cm and the characteristic relaxation time for typical nonlinear liquids is $\tau_T \sim 1$ s. For pulses of length $\tau_p \sim 10^{-8}$ s, wavelength $\lambda \sim 10^{-4}$ cm, and characteristic scale of angular structure $\theta \sim 10^{-3}-10^{-4}$ rad, heating is then an essentially nonstationary process, so that one of the mechanisms available for energy transfer is the associated stimulated temperature scattering.

A medium must have an appreciable linear or nonlinear absorption if a thermal refractive-index grating is to be produced within it. We have therefore measured the absorption coefficients of our media for different light intensities. Measurements integrated over the pulse were performed with calorimeters. The collimated light beam was passed through the cell containing the nonlinear medium. The radiation intensity remained below the level at which appreciable backscattering would be present. The resulting dependence of the transmission of the medium on the mean pulse intensity is shown in Fig. 3 for a number of media. As can be seen, nonlinear absorption was not small for the medium in which there was monotonic transfer of energy between angular components, which confirms the assumption that energy transfer occurred via the thermal mechanism. We also found that, by adding an absorbing dye ($k_\omega \sim 0.1$ cm⁻¹) to the liquid in which the distortion was nonmonotonic, e.g., to distilled water or ethyl alcohol, we were able to ensure that the deterioration in reversal became monotonic.

It is natural to assume that nonthermal energy transfer mechanisms were present in those media in which the distur-

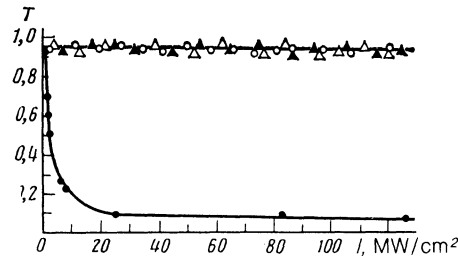


FIG. 3. Transmission coefficient T as a function of intensity I : Δ —water, Δ —acetone, \circ —ethyl alcohol, \bullet —toluene.

tion of the angular spectrum was nonmonotonic.

Of the possible redistribution mechanisms in this case, we cannot immediately exclude the orientation of anisotropic molecules ($\tau_{\text{Kerr}} \sim 10^{-12}$ s), which is an instantaneous process for nanosecond pulses. The Kerr nonlinearity can appear only for a nonlinear change in the phase of the beam.

On the other hand, in the case of striction, the attenuation time for sound of wavelength $\lambda \sim 0.1-0.01$ cm is relatively long ($\tau_s \sim 10^{-4}-10^{-5}$ s), but this in itself is not sufficient for energy transfer. The point is that SMBS is a resonance process, i.e., the interaction between the two components is effective only when the frequency difference $\Delta\omega$ between them is close enough to the frequency Ω of the sound generated by them: $|\Delta\omega - \Omega| \ll 1/\tau_s$. Consequently, the assumption that energy transfer took place on refractive-index gratings of strictional origin requires the additional frequency shift between the interacting beams. This shift can be produced by phase modulation due to the Kerr nonlinearity of the medium. Thus, the phase difference between two angular components of unequal intensity $I_{1,2}(t)$, i.e.,

$$\Delta(t) \propto n_2 [I_1(t) - I_2(t)]$$

can produce an increment $\delta\omega = \dot{\Delta}(t)$ on the frequency and can lead to the SMBS resonance:

$$\delta\omega \approx \Omega^q \equiv v_s q,$$

where n_2 is the nonlinear (Kerr) refractive index, $q = |\mathbf{k}_1 - \mathbf{k}_2|$, $I_{1,2}$ and $\mathbf{k}_{1,2}$ are the intensities and wave vectors of the two beam components, v_s is the velocity of sound in the medium, and Ω^q is the frequency of sound corresponding to the vector \mathbf{q} . As far as we know, this possibility of increasing the effectiveness of SMBS by spontaneous modulation (self-sweeping) of the pulse frequency has not been discussed in the literature.

The above experiments with the focused pump beam enabled us to establish the basic qualitative properties of energy transfer between angular components. However, quantitative studies are difficult in this experimental geometry. We therefore carried out model experiments with two collimated beams in a detailed study of the mechanisms responsible for the interaction between angular modes in nonlinear media. The experimental setup is illustrated in Fig. 4. The pump radiation was split into two beams of roughly equal intensity, and the two beams were then shaped by a lens of long focal length and were directed onto the cell in which the two beams were allowed to interact. The beam intensity ratio was varied by absorbing filters inserted into one of the beams. Coaxial photocells and the 6LOR oscillograph were used to record radiation pulses entering and leaving the cell, and to monitor stimulated backscattering.

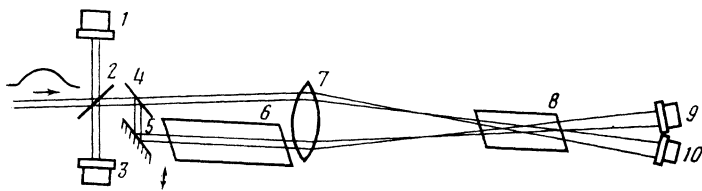


FIG. 4. Experimental setup: 1,3,9,10—photocells, 2—beam splitter, 4—semitransparent mirror, 5—100% mirror, 6—cell with Kerr medium (phase modulator), 7—lens, $f = 92$ cm, 8—interaction cell.

The working media used to investigate the thermal mechanism of energy transfer were toluene (which has nonlinear absorption; see Fig. 3) and ethyl alcohol containing a dye (linear absorption coefficient $k_\omega = 0.09 \text{ cm}^{-1}$ and transmission $T = 0.4$ over a path $l = 10$ cm). Qualitatively, the nature of the interaction with thermal gratings is the same for both linear and nonlinear absorption. Figure 5a shows oscillograms of pulses recorded with the coaxial photocells 9 and 10 (Fig. 4) in the case of thermal interaction between the beams due to linear absorption. The initial intensity ratio was $\delta^2 = 1/30$, the input intensity of the strong beam was $I_0 \approx 150 \text{ MW/cm}^2$, and the convergence angle was $\theta = 8$ mrad. As usual, the thermal interaction results in a uniform distribution of energy between the interacting components. During the pulse, the gain coefficient for the weak beams increases monotonically from zero to a maximum. As can be seen from Fig. 6, the time taken by the amplification of the weak beam to settle down decreases with increasing angle between the beams, other things being equal.

To investigate nonthermal interaction mechanisms, we selected media that did not absorb in the intensity range under investigation and had different nonlinear (Kerr) refractive indices.^{11,12} They were: acetone ($n_2 = 2.2 \times 10^{-13}$ CGSe), ethyl alcohol ($n_2 = 0.5 \times 10^{-13}$ CGSe), and distilled water ($n_2 = 0.6 \times 10^{-13}$ CGSe). In accordance with the above discussion of the nature of the strictional interaction and the contribution due to frequency self-sweeping in this process, some energy transfer was observed but only in acetone which has a high Kerr nonlinearity and, even then, only between beams of equal intensity. No energy transfer occurred in the case of equal beam intensities because the nonlinear phase gain in the two beams is the same at each instant of time, the difference between the frequencies is identically zero, and there is no SMBS resonance. On the other hand, in media with low n_2 , no energy transfer was observed at all in the intensity range used. However, when the cell containing the Kerr medium (toluene, $n_2 = 4 \times 10^{-12}$ CGSe) was introduced into the beams, along the path before the beam interaction region for beams of unequal intensity, appreciable energy transfer was produced. Energy transfer was also observed for beams of equal intensity when a Kerr cell was inserted into one of the beams.

All these facts support the strictional mechanism of energy transfer, emphasized by the Kerr quiresonance.

Figure 7a shows pulse oscillograms recorded for interacting beams of equal intensity ($I_0 \approx 150 \text{ MW/cm}^2$) in a cell filled with ethyl alcohol (convergence angle $\theta = 8$ mrad). Curve 1 corresponds to the beam into which the toluene cell was inserted ($l = 30$ cm). Curves 1 and 2 were recorded with coaxial photocells 9 and 10, respectively (see Fig. 4). There is an appreciable distortion of the temporal beam shape, and it is found that the direction of energy transfer changes several times during a pulse. For unequal input intensities (the unmodulated beam was attenuated so that the nonlinear frequency shift did not change), the temporal shape of the lower-intensity beam remained similar to that indicated by curve 2 in Fig. 7a, while the strong component was, of course, less distorted. The oscillograms of Fig. 7a were recorded as closely as possible to resonance: $\delta\omega \sim k l n_2 I_0 / \tau_i \approx \Omega^2$. When Ω^2 was reduced by a factor of two ($\theta = 4$ mrad), the beam distortion was less well defined, which may have been related to both detuning from resonance and to an increase in the settling time for the density wave. The above experiments have thus enabled us to isolate the contributions of individual nonlinear mechanisms to the energy transfer process, usually seen in a combined form. The above analysis shows that, under our conditions, which are typical for phase conjugation in liquids, many of the effects provide comparable contributions to energy transfer between the beams. The following detailed numerical model was therefore developed for the quantitative analysis of experimental data.

3. THEORY

The interaction of light with an isotropic absorbing medium is described by the following equations:^{10,13}

$$\rho_0 c_v \frac{\partial}{\partial t} \delta T - \kappa \nabla^2 \delta T - \frac{c_p - c_v}{\sigma} \frac{\partial}{\partial t} \delta \rho = \frac{n_0 c k_\omega}{4\pi} E^2, \quad (1)$$

$$\frac{\partial^2}{\partial t^2} \delta \rho - \frac{1}{\rho_0 \beta_r} \nabla^2 \delta \rho - \frac{\eta}{\rho_0} \nabla^2 \frac{\partial}{\partial t} \delta \rho - \frac{\sigma}{\beta_r} \nabla^2 \delta T = -\frac{Y}{8\pi} \nabla E^2, \quad (2)$$

$$\frac{n_0^2}{c^2} \frac{\partial^2 E}{\partial t^2} - \nabla^2 E + \frac{k_\omega n_0}{c} \frac{\partial E}{\partial t} = -\frac{1}{c^2} \frac{\partial^2}{\partial t^2} (E \delta \epsilon), \quad (3)$$

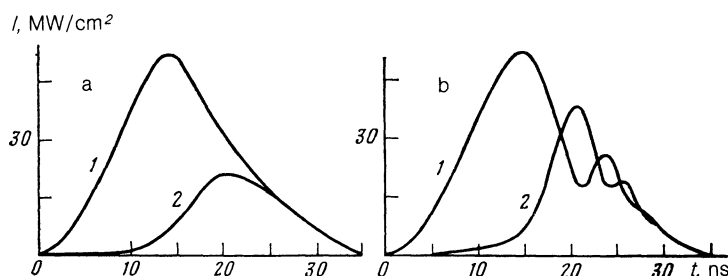


FIG. 5. Beam intensity for the thermal interaction mechanism (linear absorption): a—experiment, b—calculation; 1—strong beam, 2—weak beam. Beam convergence angle $\theta = 8$ mrad. Input beam intensity ratio $\delta^2 = 1/30$.

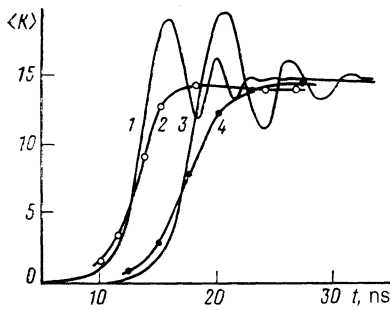


FIG. 6. Gain coefficient for the weak beam as a function of time: 1,2— $\theta = 16$ mrad, 3,4— $\theta = 8$ mrad, 1,3—calculated, 2,4—experiment. Input beam intensity ratio $\delta^2 = 1/30$.

where

$$\delta\varepsilon = \left(\frac{\partial\varepsilon}{\partial\rho}\right)_{T,\zeta} \delta\rho + \left(\frac{\partial\varepsilon}{\partial T}\right)_{\rho,\zeta} \delta T + \left(\frac{\partial\varepsilon}{\partial\zeta}\right)_{\rho,T} \delta\zeta,$$

ρ_0 is the equilibrium density of the medium, $c_{V(P)}$ is the specific heat at constant volume (pressure), κ is the thermal diffusivity, σ is the volume expansion coefficient, n_0 is the refractive index, β_T is the isothermal compressibility, η is the effective viscosity, $Y = \rho_0(\partial\varepsilon/\partial\rho)_T$ is the striction constant, E is the electric field, and $\delta\rho$, δT , $\delta\zeta$ are, respectively, the deviation of the density, temperature, and degree of orientation of the molecules from the equilibrium values.

The permittivity change $\delta\varepsilon$ responsible for scattering in the Rayleigh triplet is usually dominated by the term $(\partial\varepsilon/\partial\rho)_T$. A special investigation¹⁴ has shown that, when the term $(\partial\varepsilon/\partial T)_\rho \delta T$ is neglected, the associated error in the gain coefficient in stimulated temperature scattering is about 2–6%. Henceforth, we shall assume that¹¹ $Y \approx (n_0^2 - 1)(n_0^2 + 2)/3$. The validity of this approximation was discussed in Ref. 15. The influence of fluctuations in anisotropy will be taken into account by introducing the effective Kerr (orientational) refractive index n_2 .

For a monochromatic wave consisting of two plane components

$$E(\mathbf{r}, t) = [E_1(z, t)\exp(iqr_\perp/2) + E_2(z, t)\exp(-iqr_\perp/2)]\exp[i(\omega t - kz)] + \text{c.c.}, \quad (4)$$

with pulse length τ_p such that²⁾

$$L/c \ll \tau_p \ll \rho_0 c_p / \kappa q^2, \quad (5)$$

where L is the length of the interaction region, Eqs. (1)–(3)

yield

$$\ddot{u} + 2\gamma\dot{u} + \Omega^2 u = \frac{Yq^2}{8\pi\rho_0} E_1 E_2^* - \frac{\Omega^2 \sigma n_0 c k_\omega}{4\pi\rho_0 c_p} \int E_1 E_2^* dt', \quad (6)$$

$$i \left(\frac{\partial}{\partial z} + \frac{k_\omega}{2} \right) \begin{pmatrix} E_1 \\ E_2 \end{pmatrix} = \frac{Yk}{2n_0^2} \begin{pmatrix} E_2 u \\ E_1 u^* \end{pmatrix} + n_2 k \begin{pmatrix} |E_1|^2 + 2|E_2|^2 \\ |E_2|^2 + 2|E_1|^2 \end{pmatrix}, \quad (8)$$

where $u = \delta\rho/\rho_0$ is the relative change in density and $\gamma^{-1} = 2\rho_0/\eta q^2$ is the sound attenuation time.

We note that it is common to isolate the rapidly oscillating part in the sound equation (6), i.e., the solution is sought in the form

$$u(\mathbf{r}, t) = \bar{u}(z, t)\exp[i(\Omega t + qr_\perp)], \quad (9)$$

where $\bar{u}(z, t)$ is the slowly varying (on the scale of Ω^{-1}) sound amplitude. For large acoustic damping ($\gamma \gg 1/\tau_p$), this leads to the well-known equations for time-independent SMBS. However, for small-angle scattering ($q \ll k$), the situation can be different. Actually, when the angle between the two interacting components is $\theta \sim 10^{-3} - 10^{-2}$ rad and $k \sim 10^5$ cm⁻¹, we have $q \sim 10^2 - 10^3$ cm⁻¹ and, for $v_s \sim 10^5$ cm/s, we obtain $\Omega = v_s q \sim 10^7 - 10^8$ s⁻¹. Hence, it follows that (9) is not valid for pulses of length $10^{-7} - 10^{-8}$ s and characteristic angular structure scale of about $10^{-3} - 10^{-2}$ rad. Moreover, sound of this frequency has a very low damping constant $\gamma \ll \Omega$, since $\gamma \sim q^2$. Under these conditions, the amplitude of the sound wave is no longer proportional at each instant of time to the product of the local wave intensities, but is determined by the solution of the equation for the oscillations of a weakly-damped harmonic oscillation under the influence of an external force which acts for an interval of time of the order of the period of the natural oscillations. The frequency of this force is not constant. Thus, for $\Delta I \sim 100$ MW/cm², and $n_2 \sim 10^{12}$ cgs, the linear increase in phase over the length $l \sim 10$ cm for a pulse of $\sim 10^{-8}$ s gives $\delta\omega \sim 10^7 - 10^8$ s⁻¹, i.e., the frequency of the external force is of the order of the frequency of the natural oscillations.

Physically, the picture is as follows. Interference between the two waves induces a “light grating” in the medium, whose “lines” lie along the common direction of beam propagation. Striction or heating produces excess pressure at the interference maxima. This excess pressure tends to be released by the sound wave which begins to propagate in both directions. When the frequencies of the two components are equal, the light grating is stationary and sound generation is not very effective. However, when the phase of the light grating is a function of time, the grating moves, and

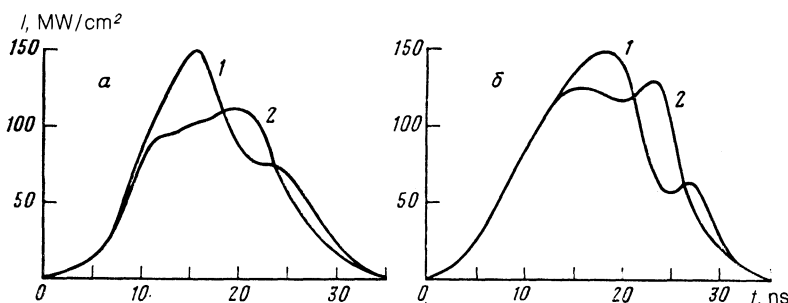


FIG. 7. Beam intensities as functions of time for the strictional mechanism with preliminary Kerr modulation of one of the beams: a—experiment, b—theory; 1—modulated beam, 2—unmodulated beam. Beam convergence angle $\theta = 8$ mrad, Kerr phase gain at pulse maximum $(\delta\varphi)_{\text{Kerr}} \approx 2\pi$.

resonance then corresponds to its displacement with the velocity of sound. In a medium with a Kerr nonlinearity, the phase gain is proportional to the distance traversed, so that the grating moves with different velocities in different cross sections. Moreover, because the Kerr increment in the frequency is determined by the derivative of the intensity, the leading and trailing edges of the pulse give rise to motion of the grating in different directions. It is not difficult to see that this relatively complex interaction picture requires detailed analysis, and the effectiveness of the above interaction can only be established by solving the complete set of equations (6)–(8).

However, these equations cannot be solved even when the analysis is confined to purely strictional interaction between the two beams that have first passed through the Kerr cell. Actually, if we write the formal solution of (6) with zero initial conditions (for $k_\omega = 0$ and $\gamma\tau_p \ll 1$)

$$u(z, t) = \frac{Yq^2}{8\pi\rho_0} \frac{1}{\Omega} \int E_1(z, t') E^*(z, t') \sin \Omega(t-t') dt', \quad (10)$$

we can reduce (7) and (8) to the form

$$\frac{\partial A_1}{\partial \xi} = iA_2 \int A_1 \sin(\tau-\tau') d\tau', \quad (11)$$

$$\frac{\partial A_2}{\partial \xi} = 2i \left[A_1 \int A_1^* \sin(\tau-\tau') d\tau' - c.c. \right] \quad (12)$$

with boundary conditions

$$\begin{aligned} A_1(\xi=0, \tau) &= \delta f(\tau) \exp[in_2 k l I_0 (1-\delta^2) f(\tau)], \\ A_2(\xi=0, \tau) &= (1-\delta^2) f(\tau). \end{aligned} \quad (13)$$

The dimensionless variables in these expressions are defined by

$$\begin{aligned} A_1 &= E_1 E_2^* / I_0, \quad A_2 = (|E_1|^2 - |E_2|^2) / I_0, \\ \xi &= (Y/16\pi n_0^2) (I_0/\rho_0 v_s^2) k z, \\ \tau &= \Omega t, \quad |E_1(0, t)|^2 = I_0 f(t), \quad |E_2(0, t)|^2 = \delta^2 I_0 f(t), \end{aligned}$$

l is the length of the cell containing the Kerr medium characterized by the refractive index n_2 , $f(t)$ describes the temporal shape of the pulse, and δ is the ratio of the amplitude of the two components, $(E_2/E_1)_{z=0}$.

It is clear that the evolution of the beam in space-time is determined by the phase relationships in the integrands of (11) and (12), which significantly depend on the temporal shape of the pulse, $f(t)$. In this situation, simple model relationships cannot be used in a general analysis of the particular experimental situation because the result is very dependent on the chosen shape of the input pulse. We therefore solved (6)–(8) numerically, having specified the pulse shape as close as possible to the experimental shape. Two separate mechanisms were investigated, namely, heating and striction with Kerr quasi-resonance.

For the numerical calculations, the set of equations given by (6)–(8), in which the Kerr nonlinearity was taken into account in the phase shift of the input beams, was reduced to a set of five first-order partial differential equations. For this set, we constructed an implicit second-order difference scheme which satisfied the Courant, Friedrichs and Lewy condition¹⁶ for convergence. To estimate the accuracy of the numerical calculations, we carried out test calculations on

successively refined meshes, and compared the sonic field $u(t, z=0)$, calculated in this way with a quadrature of (6) in which the right-hand side was known from the boundary conditions for $z=0$. The main variants were calculated for a mesh with $h_z = 0.125$ cm and $h_t = 0.25$ ns. The relative error in the calculations was a few percent.

4. RESULTS AND DISCUSSION

Calculations of the thermal interaction showed that, for transversely inhomogeneous beams, the weak component was amplified to the level of the strong component, and, thereafter, the direction of energy transfer was reversed. The gain coefficient for the weak component is given by

$$K(t) = I(L, t) / I(0, t) \exp(-k_\omega L) - 1, \quad (14)$$

and increases with time from zero to $K_{\max} = 1/\delta^2$, where δ^2 is the intensity ratio for the two components in the input beam. It then again falls to zero, and so on. At the same time, the rate of the oscillations increases with time. After a few cycles of energy transfer from the strong to the weak components and vice versa, the beam intensities become equal (the rapidly oscillating quantity is effectively averaged out at the level of 1/2). The rate of energy transfer increases with increasing intensity of the input beams for a fixed δ^2 and with decreasing grating period. This is illustrated by Table I which shows the times at which the maximum gain satisfies $K_{\max} = 1/\delta^2$ and the next minimum $K_{\min} = 0$ are reached. The calculations were performed for an interaction in the medium corresponding to the following experimental parameters (Fig. 5a): $\rho_0 = 0.789$ g/cm³, $v_s = 1.16 \times 10^5$ cm/s, $n_0 = 1.362$, $\sigma = 1.12 \times 10^{-3}$ deg⁻¹, $k_\omega = 0.09$ cm⁻¹, $c_p = 2.42 \times 10^7$ erg/g deg, $L = 10$ cm, $k = 1.19 \times 10^5$ cm⁻¹, $\delta^2 = 1/30$. The shape of the laser pulses was approximated by $f(t) \sin^2(\pi t/\tau_p)$, where $\tau_p = 35$ ns is the total pulse length.

We emphasize that the above interaction picture, with oscillations in the gain coefficient, refers to beams in which the transverse intensity distribution is constant. For a more complicated beam profile, energy transfers along directions with different intensity occur at different rates, so that the intensities of the components leaving the interaction region will obviously be given by an integral over the transverse cross section, i.e., they will be averaged. Because of the different rates of oscillations in the gain coefficient, this averaging will ensure that, under the conditions of established energy transfer, the effective gain coefficient will be lower by a factor of 2: $\langle K \rangle_{\max} = 1/2\delta^2$, i.e., the weak component will be amplified to half the level of the strong component, the intensities will equalize, and energy transfer will end.

Figure 5b shows calculated intensity profiles for the two beams at exit from the interaction region. Figure 6 shows the gain coefficients as functions of time (curves 1 and 3). It was assumed in these calculations that the lateral beam intensity distribution was Gaussian, the mean intensity of the strong component being $I_0 = 150$ MW/cm². The averaging was performed over four cross sections. The oscillations in the intensity of the beams and in the gain coefficient that can be seen on these calculated curves are entirely due to the fact that the averages were taken over discrete points and that six cross sections were not sufficient for complete smoothing. Nevertheless, the overall shape of these curves enabled us to

TABLE I. Times (in ns) to reach the first gain maximum $K_{\max} = 1/\delta$ and the next minimum $K_{\min} = 0$ (in parentheses) as functions of the intensity of the strong component (intensity ratio $\delta^2 = 1/30$ in all cases) and the angle between the beams for transversely homogeneous beams.

Angle, mrad	Pump intensity, MW/cm ²					
	25	50	75	100	125	150
4 ($\Omega\tau_p = 1$)	—(—)	—(—)	32(—)	29(—)	27(35)	26(33)
8 ($\Omega\tau_p = 2$)	32(—)	26(32)	23(28)	22(26)	21(24)	20(23)
16 ($\Omega\tau_p = 4$)	26(—)	20(24)	18(21)	17(20)	16(19)	15(18)

Note: Dash indicates that the amplification factor did not reach the maximum (or minimum) during the pulse length.

consider that the underlying model represented satisfactorily the experimental data.

Figure 7b shows the results of a calculation of the strictional interaction after preliminary Kerr modulation of one of the beams (the parameters were chosen to agree with experiment; Fig. 7a). As can be seen, there is good qualitative agreement between the numerical and experimental results. Quantitatively, the agreement lies at the limit of the precision with which stimulated backscattering could be observed ($\sim 10\%$). We note that, in the absence of nonlinear absorption, the energy balance was preserved in these experiments with the same precision. Possible channels of energy leakage would seem to include re-scattering into higher diffraction orders.¹⁷ However, estimates show that we were dealing in this case with a spatial hologram, so that the effectiveness of energy transfer to higher orders should have been low (Bragg diffraction). Actually, test calculations showed that less than 1% of the energy was lost to the first side orders.

Both calculations and experiments showed a reduction in the efficiency of energy transfer with decreasing angle between the components. In the first instance, this is due to the fact that a reduction in the angle is accompanied by an increase in the period of the light grating and, consequently, in the length of the acoustic wave produced by it. When the pulse length is less than the time taken by a phonon to traverse a distance of the order of the period of the grating, the acoustic wave does not succeed in settling down during the interaction time. Moreover, the proximity to resonance, which determines the rate of excitation of sound, plays a significant part. For example, the intensity of the acoustic field at $\theta = 8$ mrad (optimum) is greater by an order of magnitude than at $\theta = 4$ mrad.

It is clear from Fig. 7 that the main distortions occur near the pulse center. This is so because an appreciable growth of the density wave begins when the phase difference between the induced sound wave and the inducing force (light grating) reaches the optimum value of $\pi/2$. The phase of the sound wave is stabilized near the pulse center when the light grating, which at first moves with an increasing, and then a decreasing, velocity, begins to lag behind the induced sound wave.

Transverse averaging also plays an important part in this case because portions of the pulse of different intensity enter into resonance with different angular components. Hence, as in the case of the thermal interaction, averaging leads to appreciable smoothing of pulsations during energy transfer.

In conclusion, let us compare the relative contributions

of the two mechanisms to the distortion of the angular structure of the beam, using simple estimates of the growth rates of the weak angular components. For the thermal mechanism,

$$g^T(\Omega\tau_p \gg 1) \approx g_0^T = Yk \frac{\sigma k_\omega}{\rho_0 n_0 c_p} \frac{c}{8\pi} |E_0|^2 \tau_p, \quad (15)$$

$$g^T(\Omega\tau_p \lesssim 1) \approx (\Omega\tau_p)^2 g_0^T,$$

and for striction

$$g^{\text{str}} \approx g_{\text{opt}}^{\text{str}} \begin{cases} (\Omega\tau_p) \Delta, & \Omega\tau_p \lesssim 1, & \Delta \lesssim 1 \\ 1/\Omega\tau_p, & \Omega\tau_p \gg 1, & \Delta \ll \Omega\tau_p \\ 1/\Delta, & \Delta \gg 1, & \Omega\tau_p \ll \Delta \end{cases} \quad (16)$$

where

$$g_{\text{opt}}^{\text{str}} = \frac{Y^2 k}{16\pi n_0^2} \left(\frac{|E_0|^2}{\rho_0 v_s^2} \right) \Omega\tau_p$$

is the optimum growth rate for $\Omega\tau_p \gg 1$ and $|\Delta - \Omega\tau_p| \ll 1$. These estimates yield the following ratio for the two mechanisms:

$$\frac{g^{\text{str}}}{g^T} \approx \frac{Y}{n_0} \frac{c_p}{\sigma c k_\omega v_s^2} \begin{cases} \Delta/\tau_p, & \Omega\tau_p \lesssim 1, & \Delta \lesssim 1, \\ \Omega, & \Omega\tau_p \gg 1, & \text{resonance} \\ 1/\tau_p, & \Omega\tau_p \gg 1, & \text{no resonance} \end{cases} \quad (17)$$

We must now take into account the fact that, when a volume ΔV of the liquid absorbs an amount $\rho_0 c_p T \Delta V$ of heat, all the particles in this volume acquire velocities of the order of the acoustic velocity, i.e., $\rho_0 T \sim \rho_0 v_s^2$, so that the relative change in the volume is $\delta V/V = \sigma T \sim 1$. This enables us to write (17) in the following more convenient form:

$$\frac{g^{\text{str}}}{g^T} \approx \frac{Y}{n_0} \frac{1}{c k_\omega} \begin{cases} \Delta/\tau_p, & \Omega\tau_p \lesssim 1, & \Delta \lesssim 1, \\ \Omega, & \Omega\tau_p \gg 1, & \text{resonance} \\ 1/\tau_p, & \Omega\tau_p \gg 1, & \text{no resonance} \end{cases} \quad (18)$$

Hence, it follows that, when $k_\omega \gtrsim k\theta v_s/s$, where θ is the characteristic angular size of the beam, thermal distortions predominate even when the optimal conditions for the strictional mechanism are satisfied. Conversely, when $k_\omega \lesssim \min(1/c\tau_p, k\theta v_s/c)$ the main contribution to beam distortion is provided by striction.

It is interesting to compare the growth rates (15) and (16) with the growth rate for stimulated Mandel'shtam-Brillouin backscattering:

$$g_{\text{SMBs}}^{180^\circ} = Y^2 k^2 |E_0|^2 / 16\pi n_0^2 \rho_0 v_s \gamma^{180^\circ},$$

where $1/\gamma^{180^\circ}$ is the attenuation time for sound of frequency

$2kv_s$. We then have

$$g_{\text{opt}}^{\text{str}} \sim g_{\text{SMBS}}^{180^\circ} \gamma^{180^\circ} \tau_p \theta, \quad (19)$$

$$g_0^T \sim g_{\text{SMBS}}^{180^\circ} \frac{k_\omega}{k} \frac{c}{v_s} \gamma^{180^\circ} \tau_p. \quad (20)$$

Since the exponential factor $g_{\text{SMBS}}^{180^\circ} L$ must reach ≈ 25 if stimulated Mandel'shtam-Brillouin backscattering is to develop above the noise level, and beam distortion is already present for $g^{\text{str}(T)} L \sim 1$, we find from (19) and (20) that good phase conjugation can be achieved for

$$(\gamma^{180^\circ} \tau_p) \theta \lesssim 1/25,$$

if SMBS is excited in a nonabsorbing medium with Kerr nonlinearity, or when

$$\frac{k_\omega}{k} \frac{c}{v_s} (\gamma^{180^\circ} \tau_p) \lesssim 1/25$$

in an absorbing medium with small Kerr nonlinearity.

The estimates given by (19) and (20) were obtained for the situation that was optimal for the development of distortions. On the other hand, if the pulse length τ_p and the angular size θ of the beam are such that $\theta \tau_p \lesssim 1/v_s k$ (i.e., $\Omega \tau_p \lesssim 1$), or the condition for the Kerr resonance in one of the angular components of the beam is satisfied, conditions (19) and (20) are correspondingly relaxed [see (15) and (16)].

5. CONCLUSION

Our research shows that, when beams with a complicated angular structure propagate in nonlinear media, their angular spectrum may undergo appreciable distortion. There are two reasons for this: absorption in the medium and electrostriction, the latter being emphasized by the Kerr quasi-resonance. The thermal mechanism gives rise to the development of weak angular modes due to the strong central component and the uniform angular energy distribution in the beam, whereas the strictional mechanism and the Kerr nonlinearity together produce a significant distortion of the temporal shape of the angular modes for which the resonance conditions are satisfied, even though they do not produce a large amplification of the weak components.

The theoretical model used in this research is in good agreement with experimental data, but the results indicate that each specific situation requires careful analysis when all the characteristic times of the problem are of the same order. The propagation and distortion of the beam are strongly influenced by the temporal shape and the duration of pulses, the angular composition of the beam, and the parameters of the medium. Nevertheless, our results enable us to formulate the following quite general recommendations.

1. Both heating and striction distort mostly the large-angle part of the distribution $\theta > \theta_{\text{thr}}$, where the width θ_{thr} of the undistorted region depends on the pulse length as follows:

$$\theta_{\text{th}} \sim \lambda / \tau_p v_s.$$

2. The thermal mechanism produces a uniform broadening of the angular spectrum of the beam for $\theta > \theta_{\text{thr}}$. The strictional mechanism has a well-defined resonance, $\theta_{\text{opt}} \sim \theta_{\text{thr}} \Delta$, and its effectiveness increases with increasing angle under resonance conditions.

3. Thermal distortions can be reduced, of course, by using media with low absorption, or by reducing the pulse length in inverse proportion to the width θ of the angular spectrum of the beam:

$$\tau_p \lesssim \lambda / v_s \theta.$$

Satisfactory phase conjugation can be achieved with SMBS by ensuring that the absorption coefficient of the medium satisfies the condition

$$k_\omega < \frac{1}{25} k \frac{v_s}{c} \frac{\tau_{\text{ph}}}{\tau_p}$$

(τ_{ph} is the lifetime of phonons of frequency $2kv_s$).

4. Strictional distortions can be reduced by using media with low Kerr nonlinearity, so that the nonlinear phase gain is small, $\Delta \lesssim 1$. On the other hand, when $\Delta \gg 1$, strictional distortions can be suppressed by reducing the pulse length down to $\lambda / v_s \theta$. In media with well defined Kerr nonlinearity, satisfactory phase conjugation can be achieved only for pulses whose length and angular spectrum satisfy the condition $\theta \tau_s < \tau_{\text{ph}} / 25$.

¹⁰We shall not consider the electrocaloric effect because it usually appears together with striction, but its contribution is appreciably smaller¹⁰: $(\partial \epsilon / \partial T)_\rho \delta T \ll (\partial \epsilon / \partial \rho)_T \delta \rho$.

¹¹The right-hand side of (5) enables us to neglect thermal diffusivity, and the left-hand side enables us to discard the time derivatives in the field equation (3) (this is the so-called thin-layer approximation).

¹V. L. Vinetskiĭ, N. V. Kukhtarev, S. G. Odulov, and M. S. Soskin, *Usp. Fiz. Nauk* **129**, 113 (1979) [*Sov. Phys. Usp.* **22**, 742 (1979)].

²A. V. Groznyi, A. M. Dukhovnyi, A. A. Leshchev *et al.*, in: *Opticheskaya golografiya* (in: *Optical Holography*), Nauka, Leningrad, 1979, p. 92.

³V. N. Belousov, L. A. Bolpshov, N. G. Koval'skiĭ, and Yu. K. Nizienko, *Zh. Eksp. Teor. Fiz.* **79**, 2119 (1980) [*Sov. Phys. JETP* **52**, 1071 (1980)]. *Proc. Intern. Conf. on Lasers '81*, Dec. 14–18, 1981, New Orleans, 1981; Collection, p. 176, Ref. 7.

⁴K. S. Gochelashvili, I. V. Chashei, and V. I. Shishov, *Kvantovaya Elektron. (Moscow)* **7**, 2077 (1980) [*Sov. J. Quantum Electron.* **10**, 1207 (1980)].

⁵A. R. Bogdan, Y. Prior, and N. Blombergen, *Opt. Lett.* **6**, 82 (1981).

⁶L. A. Bol'shov, D. V. Vlasov, and R. A. Garaev, *Kvantovaya Elektron. (Moscow)* **9**, 83 (1982) [*Sov. J. Quantum Electron.* **12**, 52 (1982)].

⁷Yu. I. Kucherov, S. A. Lesnik, M. S. Soskin, and A. I. Khizhnyak, B sb. *Obrazhenie volnovogo fronta izlucheniya v nelineinykh sredakh* (in: *Wavefront Reversal in Nonlinear Media*), IPF AN SSSR, Gorki, 1982, p. 111.

⁸M. V. Vasil'ev, V. Yu. Venediktov, A. A. Leshchev *et al.*, *Zh. Tekh. Fiz.* **53**, 1979 (1983) [*Sov. Phys. Tech. Phys.* **28**, 1216 (1983)]. V. Yu. Venediktov, L. B. Lalyko, A. A. Leshchev, and V. G. Sidorovich, *Zh. Tekh. Fiz. Lett.* **10**, 401 (1984) [*Sov. Tech. Phys. Lett.* **10**, 168 (1984)].

⁹V. I. Bespalov, E. L. Bubis, O. V. Kulagin *et al.*, *Tezisy dokladov XII Vsesoyuznoi konferentsii po kogerentnoi i nelineinoy optike* (Abstracts of Papers read to the Twelfth All-Union Conf. on Coherent and Nonlinear Optics), Moscow, 1985, p. 585.

¹⁰V. S. Starunov and I. L. Fabelinskiĭ, *Usp. Fiz. Nauk* **98**, 441 (1969) [*Sov. Phys. Usp.* **12**, 463 (1970)].

¹¹Y. R. Shen, *Phys. Lett.* **20**, 378 (1966).

¹²R. W. Hellwarth, *Prog. Quantum Electron.* **5**, 1 (1977).

¹³I. P. Batra, R. H. Enns, and D. Pohl, *Phys. Status Solidi B* **48**, 11 (1971).

¹⁴I. P. Batra and R. H. Enns, *Phys. Rev.* **185**, 396 (1969).

¹⁵D. J. Soumou, E. L. Mackor, and J. Hijmans, *Trans. Faraday Soc.* **60**, 1539 (1964).

¹⁶S. K. Godunov, and V. S. Ryaben'kiĭ, *Raznostnye skhemy* (Difference Schemes), Nauka, Moscow, 1973.

¹⁷S. S. Rangnekar and R. H. Enns, *Can. J. Phys.* **52**, 99 (1974).

Translated by S. Chomet